

A New Trend for FET Small Signal Modeling Using Cepstral Analysis

R. R. Elsharkawy¹

S. El-Rabie²

M. Hindy¹

M. I. Dessouky²

¹Institute of Electronics Research,
Cairo.
EGYPT.

²Department of Electronics and Electrical Communications,
Faculty of Electronic Engineering, 32952, Menouf.
EGYPT.

correo electrónico (email): raniarefaat85@yahoo.com
srabie1@yahoo.com
m1_hendi@yahoo.com
dr_moawad@yahoo.com

Recibido el 8 de septiembre de 2010; aceptado el 16 de marzo de 2011.

1. Abstract

In this paper, a new technique is proposed for field effect transistor (FET) small-signal modeling using neural networks. This technique is based on the combination of the Mel-frequency Cepstral Coefficients (MFCCs) with the different discrete transforms such as the discrete cosine transform (DCT), the discrete sine transform (DST), and the discrete wavelet transform (DWT) of the inputs to the neural networks. The input data sets to traditional neural systems for FET small-signal modeling are the scattering parameters and the corresponding frequencies in a certain band, and the outputs are the circuit elements. In the proposed approach, these data sets are considered as forming random signals. The MFCCs of the random signals are used to generate a small number of features characterizing the signals. In addition, other vectors are calculated from the DCT, the DST, or the DWT of the random signals and appended to the MFCCs vectors calculated from signals. The new feature vectors are used to train the neural networks. The objective of using these new vectors is to characterize the random input sequences with much more features to be robust against measurement errors. There are two benefits

for these approaches: a reduction in the number of neural networks input, hence a faster convergence of the neural training algorithm and robustness against measurement errors in the testing phase. Experimental results show that the techniques based on the discrete transforms are less sensitive to measurement errors than using the traditional and MFCCs methods.

Key words: MFCCs, Neural networks, DST, FET, DWT, DCT.

2. Resumen (Nueva técnica para el transistor de efecto de campo (FET) de pequeña señal modelado con redes neuronales)

En este trabajo se propone una nueva técnica para el transistor de efecto de campo (FET) de pequeña señal de modelado con redes neuronales. Esta técnica se basa en la combinación de los coeficientes de frecuencia Mel Cepstral (MFCC) con las diferentes transformaciones discretas, tales como la transformada discreta del coseno (DCT), la transformada discreta del seno (DST), y la transformada discreta wavelet (DWT) de la entrada a las redes neuronales. Los datos de entrada a los sistemas tradicionales conjuntos neuronales para el FET de pequeña señal de modelado son los parámetros de dispersión y las frecuencias correspondientes en una determinada banda, y las salidas son los elementos del circuito. En el enfoque propuesto, este conjunto de datos son considerados como constitutivos de señales aleatorias. El MFCC de las señales aleatorias se utiliza para generar un pequeño número de rasgos que caracterizan las señales. Además, otros vectores se calculan a partir de la DCT, de DST, o la DWT de la señal al azar y se añade a los vectores MFCC calculados a partir de las señales. Los vectores de características nuevas se utilizan para entrenar las redes neuronales. El objetivo de la utilización de estos nuevos vectores es la caracterización de las secuencias de entrada al azar con características mucho más para ser robustos frente a errores de medición. Hay dos ventajas de estos enfoques, una reducción en el número de entradas de las redes neuronales y, por lo tanto, una convergencia más rápida del algoritmo de entrenamiento neural y robustez frente a errores de medición en la fase de pruebas. Los resultados experimentales muestran que las técnicas basadas en las transformaciones discretas son menos sensibles a los errores de medición que el uso de los métodos tradicionales y MFCC.

Palabras clave: MFCC, redes neuronales, DST, DWT FET, DCT.

3. Introduction

Knowledge of the equivalent circuit of a FET is very useful for the device performance analysis. Therefore, it is very important to use efficient tools to predict the small-signal circuit elements. Two major solution categories have been proposed by researchers to solve the small-signal modelling problem of transistors. The first trend is based on the direct extraction of small-signal circuit elements through analytic solutions [1-4]. This trend is very complicated, because it depends on finding closed form expressions to relate the scattering parameters of the FET to the small-signal circuit elements.

The second trend is directed towards optimizing the component values to closely fit the small-signal microwave scattering parameters measured or published for the device [5-8]. However, the equivalent circuit determination needs accurate broad-band S-parameters measurements. In fact, there are inherent errors in vector network analyzer measurements, which can not be avoided easily. Therefore, there is a need for a new approach, which is more robust to errors in the scattering parameters measurements.

Several modeling approaches based on artificial neural networks and belonging to the second category of solutions have been presented in literature [9-11]. Neural networks have the ability to simulate nonlinear relations with high accuracy. They can achieve a trade-off between efficiency and accuracy. Based on these advantages of neural networks, they found a great popularity in modeling the nonlinear relations between the measured or published FET scattering parameters and the values of the small-signal circuit elements. The traditional approach for this purpose is to build a single neural network to relate all the measured scattering parameters to the small-signal circuit elements, but this approach is time consuming and does not guarantee convergence in the training phase of the neural network.

In this paper, the MFCCs of the neural inputs in the traditional method and the MFCCs of their DCTs, DSTs, and DWTs are extracted and concatenated to form feature vectors to be used as the new neural input vectors. The paper presents a study of the sensitivity of the traditional and the proposed neural models to measurement errors in the testing phase. The paper is organized as follows. Section 4 gives the basics of neural small-signal modeling. Section 5 gives the small-signal model for the metal semiconductor field effect transistor (MESFET) that will be used throughout the paper. Section 6 presents the proposed technique for FET small-signal modeling. Section 7 gives the experimental results. Finally, Section 8 gives the concluding remarks.

4. Neural small-signal modeling

Artificial neural networks are programming paradigms that seek to emulate the microstructure of the brain, and they are used extensively in artificial intelligence problems from simple pattern-recognition tasks to advanced symbolic manipulation. Generally, artificial neural networks are basic input and output devices, with the neurons organized in layers. They have the ability to model nonlinear relations such as the relations between the scattering parameters and the small-signal circuit elements in FETs. Several neural structures can be implemented for this purpose. The multilayer perceptron (MLP) network is one of such configurations [12,13]. It is a feed-forward artificial neural network that maps sets of input data onto a set of appropriate outputs. A standard MLP neural network is shown in Fig. 1. It consists of an input and an output layer with one or more hidden layers of nonlinearly-activated nodes. Each node in a layer connects with a certain weight w_{ij} to every other node in the following layer, but there are no connections between the same layer neurons.

An MLP with one hidden layer can be used for FET small-signal modeling. The sigmoid function $F(u) = 1/(1 + e^{-u})$ can be used as an activation function for the hidden layer, and the neurons from the input and output layers can have linear activation functions. Let \mathbf{X} be the input vector to a single hidden layer neural network, the output vector \mathbf{Y} can be obtained according to the following matrix equation [12, 13]:

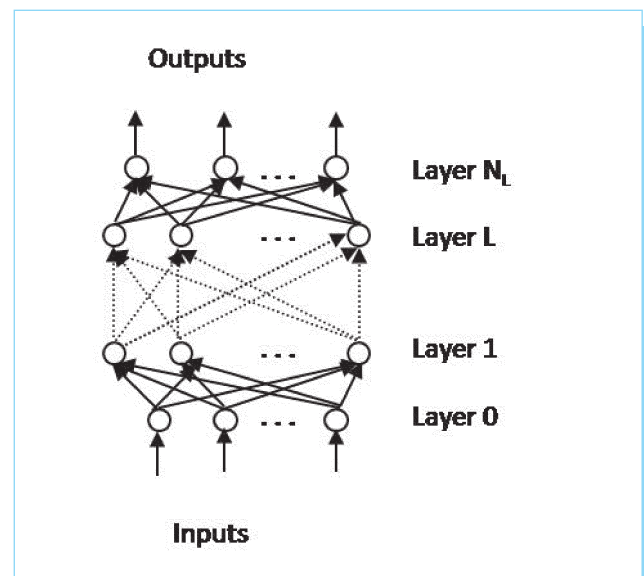


Fig. 1. Standard MLP neural network.

$$Y = W_2 * F(W_1 * X + B_1) + B_2 \quad (1)$$

where W_1 and W_2 are weight matrices between the input layer and the hidden layer and between the hidden layer and the output layer, respectively. B_1 and B_2 are bias matrices for the hidden layer and the output layer, respectively. The neural network learns the relationship among sets of input/output data (training sets), that represents the characteristics of the component under consideration. First, input vectors are presented to the input neurons and output vectors are computed. These output vectors are then compared with desired values and errors are computed. Error derivatives are calculated and summed up for each weight and bias until the whole training set has been presented to the network. These error derivatives are then used to update the weights and biases for neurons in the model. The training process proceeds until errors become lower than the prescribed values or until the maximum number of epochs is reached. Once a neural network is trained, its structure remains unchanged, and it will be capable of predicting outputs for all inputs whether they have been used for the training or not.

5. FET small-signal models

Many researchers are interested in FET small-signal modeling. They introduced several models. Of such models, the model of the Mimix CF001-01 MESFET published in its datasheet in 2008. This model is illustrated in Fig. 2. This model is valid up to 26 GHz.

6. Proposed neural modeling techniques

A direct approach to generate a neural model for a MESFET is to use the frequency values, the magnitude and the phase of the S-parameters as inputs to a single MLP neural network and the circuit elements as the outputs. In the proposed techniques, we take the parameters of the CF001-01 MESFET shown in Table 1 as inputs to several neural networks and the circuit elements as outputs for each network, separately. A training process can be performed with these data sets or other data sets.

Table (1) Published S-parameters for which, the values of the small-signal elements of the CF001-01 are given by $L_g = 0.19$ nH, $R_g = 1$ Ω , $C_{gs} = 0.32$ pF, $R_i = 1.9$ Ω , $C_{gd} = 0.023$ pF, $G_m = 66$ mS, $\tau = 2.7$

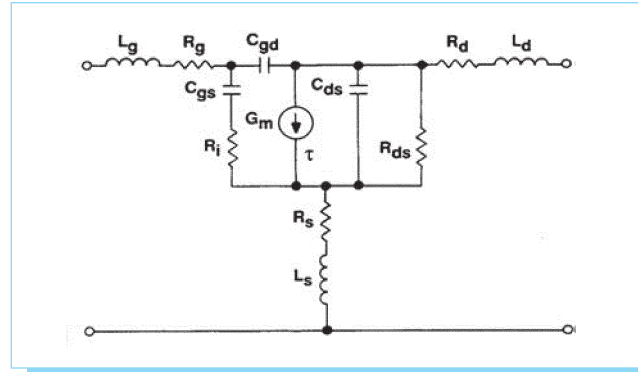


Fig. 2. The model of CF001-01MESFET.

ps, $C_{ds} = 0.12$ pF, $R_{ds} = 161$ Ω , $R_d = 1.3$ Ω , $L_d = 0.21$ nH, $R_s = 1.1$ Ω , $L_s = 0.04$ nH.

Using all the data in Table 1 as inputs for the neural network and the circuit elements as outputs in a single neural structure as in the traditional methods causes two problems. First problem is that the amount of data will be very large. Second one is that the convergence will not be guaranteed. Thus, all the proposed techniques will be used to achieve convergence and reduce the amount of input data. The steps of the proposed techniques can be summarized as follows:

1. Calculate the MFCCs for the original input data considering it as a random signal.

Table 1. S-parameters for which, the values of the small-signal elements of the CF001-01.

f (GHz)	S_{11}		S_{21}		S_{12}		S_{22}	
	Mag.	Angle	Mag.	Angle	Mag.	Angle	Mag.	Angle
2	0.98	-24°	4.56	156°	0.02	73°	0.53	-10°
4	0.93	-51°	4.31	136°	0.04	62°	0.5	-25°
6	0.88	-72°	3.83	118°	0.05	51°	0.48	-35°
8	0.84	-98°	3.47	100°	0.06	38°	0.43	-51°
10	0.79	-122°	2.99	82°	0.06	23°	0.38	-68°
12	0.79	-140°	2.64	67°	0.07	18°	0.38	-83°
14	0.78	-154°	2.41	55°	0.07	10°	0.39	-93°
16	0.78	-166°	2.27	44°	0.07	5°	0.36	-101°
18	0.77	178°	2.16	30°	0.08	-2°	0.32	-113°
20	0.76	159°	2.04	15°	0.09	-13°	0.27	-131°
22	0.79	141°	1.82	-2°	0.09	-20°	0.27	-163°
24	0.78	132°	1.52	-13°	0.09	-21°	0.3	176°
26	0.81	129°	1.31	-21°	0.09	-19°	0.39	168°

2. Calculate the DCT, DST or DWT for the original data.
3. Calculate the MFCCs for the outputs of step 2.
4. Make a concatenation between the two vectors obtained from steps 1 and 3.
5. In the training phase, use the output of step 4 with each circuit element of the training set to train a neural network belonging to this element.
6. In the testing phase, steps 1 to 4 are performed on the measured S-parameters with measurement errors and the resulting vectors are used to predict the circuit elements with their neural networks.

The MFCC technique is used to reduce the amount of input data as all the inputs are replaced by a small number of MFCC. Measurement errors are similar in nature to random noise. It is known in speaker identification, that the MFCC can be used to characterize speech signals in the presence of noise rather than using all the signal samples in the identification process. The same idea is exploited here considering the measurement errors as noise. Extracting the MFCC from the DCT, DST or DWT of the neural inputs can add more features to characterize the neural inputs in the presence of measurement errors leading to more robust modeling.

6.1. The discrete cosine transform

The DCT expresses a sequence of finite data points in terms of a sum of cosine functions oscillating at different cosine frequencies. It is defined for a sequence of samples $x(n)$ by the following equation [14]:

$$X(k) = w(k) \sum_{n=0}^{N-1} x(n) \cos \left[\frac{\pi(2n-1)(k-1)}{2N} \right] \quad k = 0, \dots, N-1 \quad (2)$$

where

$$w(k) = \begin{cases} \frac{1}{\sqrt{N}} & k = 0 \\ \sqrt{\frac{2}{N}} & k = 1, \dots, N-1 \end{cases}$$

The DCT has a sophisticated characteristic of energy compaction by collecting most of the signal energy in a few samples leaving the other samples very small. This characteristic can be exploited in our work to reduce the effect of measurement errors.

6.2. The discrete sine transform

The DST is a mathematical transform that uses sine functions oscillating at different frequencies to transform time signals into a different domain. It is defined a sequence of samples $x(n)$ by the following equation [14-16]:

$$X(k) = \sum_{n=0}^{N-1} x(n) \sin \left[\frac{\pi kn}{N+1} \right] \quad k = 0, \dots, N-1 \quad (3)$$

The MFCC will be extracted from $X(k)$ to add more features to those extracted from $x(n)$. The concatenation of the feature vectors extracted from $x(n)$ and $X(k)$ will give a more robust feature vector to characterize $x(n)$, even in the presence of measurement errors in the testing phase.

6.3. The discrete wavelet transform

The DWT is a very popular tool for the analysis of non-stationary signals. It can be regarded as equivalent to filtering the signal with a bank of bandpass filters, whose impulse responses are all approximately given by scaled versions of a mother wavelet. The scaling factor between adjacent filters is usually 2:1 leading to octave bandwidths and center frequencies that are one octave apart [17-30]. The outputs of the filters are usually maximally decimated so that the number of DWT output samples equals the number of input samples, and thus no redundancy occurs in this transform. The one level DWT decomposition-reconstruction filter bank is shown in Fig. 3.

The art of finding a good wavelet lies in the design of the set of filters H_0, H_1, G_0 and G_1 to achieve various tradeoffs between spatial and frequency domain characteristics while

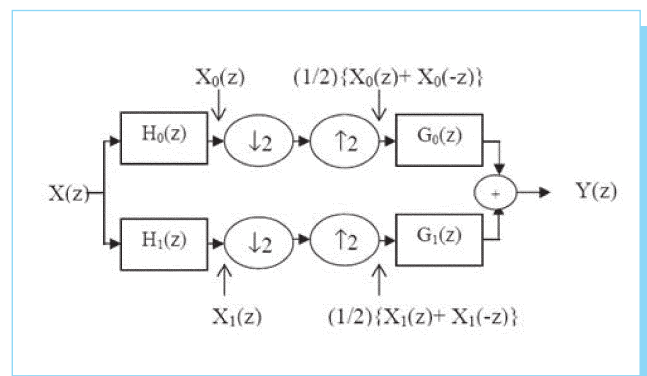


Fig. 3. The two band decomposition-reconstruction wavelet filter bank.

satisfying the perfect reconstruction (PR) condition [29]. In Fig. 3, the process of decimation and interpolation by 2:1 at the output of H_0 and H_1 effectively sets all odd samples of these signals to zero. For the lowpass branch, this is equivalent to multiplying $x_0(n)$ by $1/2(1 + (-1)^n)$. Hence $X_0(z)$ is converted to $1/2\{X_0(z) + X_0(-z)\}$. Similarly, $X_1(z)$ is converted to $1/2\{X_1(z) + X_1(-z)\}$.

Thus, the expression for $Y(z)$ is given by [29]:

$$\begin{aligned} Y(z) &= \frac{1}{2}\{X_0(z) + X_0(-z)\}G_0(z) + \frac{1}{2}\{X_1(z) + X_1(-z)\}G_1(z) \\ &= \frac{1}{2}X(z)\{H_0(z)G_0(z) + H_1(z)G_1(z)\} \\ &\quad + \frac{1}{2}X(-z)\{H_0(-z)G_0(z) + H_1(-z)G_1(z)\} \end{aligned} \quad (4)$$

The first PR condition requires aliasing cancellation and forces the above term in $X(-z)$ to be zero. Hence,

$$\{H_0(-z)G_0(z) + H_1(-z)G_1(z)\}=0,$$

which can be achieved if [29]:

$$H_1(z) = z^k G_0(-z) \text{ and } G_1(z) = z^k H_0(-z) \quad (5)$$

where k must be odd (usually $k = \pm 1$).

The second PR condition is that the transfer function from $X(z)$ to $Y(z)$ should be unity [26]:

$$\{H_0(z)G_0(z) + H_1(z)G_1(z)\}= 2 \quad (6)$$

If we define a product filter $P(z) = H_0(z)G_0(z)$ and substitute from Eq. (5) into Eq. (6), then the PR condition becomes [29]:

$$H_0(z)G_0(z) + H_1(z)G_1(z)\}= P(z) + P(-z) = 2 \quad (7)$$

This needs to be true for all z and, since the odd powers of z in $P(z)$ cancel with those in $P(-z)$, it requires that $p_0 = 1$ and $p_n = 0$ that for all n even and non-zero. The polynomial $P(z)$ should be a zero phase polynomial to minimize distortion. In general, $P(z)$ is of the following form [29]:

$$P(z) = \dots + p_5 z^5 + p_3 z^3 + p_1 z + 1 + p_1 z^{-1} + p_3 z^{-3} + p_5 z^{-5} + \dots \quad (8)$$

The design method for the PR filters can be summarized in the following steps [26]:

1. Choose p_1, p_3, p_5, \dots to give a zero phase polynomial $P(z)$ with good characteristics.
2. Factorize $P(z)$ into $H_0(z)$ and $G_0(z)$ with similar lowpass frequency responses.

3. Calculate $H_1(z)$ and $G_1(z)$ from $H_0(z)$ and $G_0(z)$.

To simplify this procedure, we can use the following relation:

$$P(z) = P(Z) = 1 + p_{t,1}Z + p_{t,3}Z^3 + p_{t,5}Z^5 + \dots \quad (9)$$

where $Z = 1/2 (z + z^{-1})$

The Haar wavelet is the simplest type of wavelets. In the discrete form, Haar wavelets are related to a mathematical operation called the Haar transform. The Haar transform serves as a prototype for all other wavelet transforms [26]. Like all wavelet transforms, the Haar transform decomposes a discrete signal into two sub-signals of half its length. One sub-signal is a running average or trend; the other sub-signal is a running difference or fluctuation. This uses the simplest possible $P_c(Z)$ with a single zero at $Z = -1$. It is represented as follows [29]:

$$P_c(Z) = 1+Z \text{ and } Z = 1/2 (z + z^{-1}) \quad (11)$$

thus

$$P(z) = 1/2 (z + 2 + z^{-1}) = 1/2 (z + 1)(1 + z^{-1}) = G_0(z)H_0(z) \quad (12)$$

We can find $H_0(z)$ and $G_0(z)$ as follows:

$$H_0(z) = 1/2 (1 + z^{-1}) \quad (13)$$

$$G_0(z) = (z + 1) \quad (14)$$

Using Eq.(5) with $k=1$:

$$G_1(z) = zH_0(-z) = 1/2 z(1 + z^{-1}) = 1/2 (z - 1) \quad (15)$$

$$H_1(z) = z^{-1}G_0(-z) = z^{-1}(-z + 1) = (z^{-1} - 1) \quad (16)$$

The two outputs of $H_0(z)$ and $H_1(z)$ are concatenated to form a single vector of the same length as the original input signal. The features are extracted from this vector and added to the feature vector generated from the original input signal to form a large feature vector. The wavelet transformed signal vector contains both the approximation and the detail coefficients of the input signal formed from the neural inputs. So, feature extraction from this vector gives features from the lowpass as well as the highpass components of the signal which are more robust features to the presence of measurement errors.

6.4. Extraction of the MFCC

The MFCC of a data sequence are a representation of the short-term coefficients derived from a type of cepstral transformation of this data sequence. Calculating the MFCCs of

a data sequence $x(n)$, the DFT of the sequence is computed to obtain the magnitude spectrum as follows [31,32]:

$$X(k) = \sum_{n=0}^{N-1} x(n)e^{-j2\pi kn/N} \quad (17)$$

The magnitude spectrum $|X(k)|$ is now scaled in both frequency and magnitude. First, the frequency is scaled logarithmically using the so-called Mel filter bank $H(k,m)$, and then the logarithm is taken, giving:

$$X'(k) = \ln \left[\sum_{k=0}^{N-1} |X(k)|H(k,m) \right] \quad (18)$$

for $m=1, 2, \dots, M$, where M is the number of filter banks and $M \ll N$.

The Mel filter bank is a collection of triangular filters defined by center frequencies calculated on the Mel scale [31,32]. The triangular filters are spread over the entire frequency range from zero to the Nyquist frequency. Finally, the MFCCs are obtained by computing the DCT of using [31,32]:

$$c_l = \sum_{m=1}^M X'(m) \cos \left[l \frac{\pi}{M} \left[m - \frac{1}{2} \right] \right] \quad (19)$$

7. Experimental results

In this section, several experiments are carried out to test the proposed techniques for FET small-signal modeling. The

experiments are carried out on the CF001-01 GaAs MESFET model. The published S-parameters for this model are tabulated in Table 1.

Five methods are tested for creating neural models to estimate the small-signal circuit elements from the published parameters. These methods are the traditional neural network modeling method using all published data as inputs, the proposed method using the MFCCs of the published data, and the proposed methods using a concatenation of the MFCCs obtained from the original data and the MFCCs obtained from one of the discrete transforms; the DCT, the DST or the DWT of this data.

For all the experiments, a neural network is created through training to relate each circuit element to the neural inputs, whether they are the published data or features extracted from this data.

The number of epochs required in the training phase for each method are tabulated in Tables 2 and 3. From these tables, it is clear that the number of epochs required for creating the neural networks is lower for the discrete transforms methods than that for the traditional method in most cases, which reveals that the proposed methods are time saving.

In the testing phase, the neural networks are tested with input data subject to measurement errors. The measurement errors are simulated as uniformly distributed random errors added to the published data. A comparison study is held between the sensitivity of the five methods to the measurement errors in the published parameters. The results of this comparison study for all elements are given in Fig.(4) from (a) to (m). In these experiments, each circuit element is estimated using its created neural networks for all methods with errors having a uniform distribution added to the neural inputs. Since the errors in all neural inputs are not fixed, the maximum percentage error among the neural inputs is taken as the horizontal axis and the percentage error in the estimated value of the circuit element is taken as the vertical axis.

Figure 4 shows that the methods based on the MFCCs with the discrete transforms of the inputs are more robust to measurement errors than the traditional method and MFCCs method only. We notice from the figure that the use of the MFCCs with the DCT is the best method for most cases.

Table 2. The number of epochs required in each method for the intrinsic elements of the CF001-01 model.

Method of Estimation	C_{ga}	R_i	C_{gd}	g_m	τ	C_{da}	R_{da}
Traditional Method	2315	239	800	1050	1199	1349	815
MFCC Method	463	9	311	500	17	2017	167
DCT Method	13	20	1210	931	5	884	91
DST Method	11	172	28	445	4	15	15
DWT Method	13	100	557	97	6	534	10 000

Table 3. The number of epochs required in each method for the extrinsic elements of the CF001-01 model.

Method of Estimation	L_g	R_g	L_d	R_d	L_s	R_s
Traditional Method	1457	310	1860	3044	889	3250
MFCC Method	700	28	2448	16	451	258
DCT Method	10	9	6	2487	580	5
DST Method	24	235	117	13	11	9
DWT Method	33	10	39	6	603	15

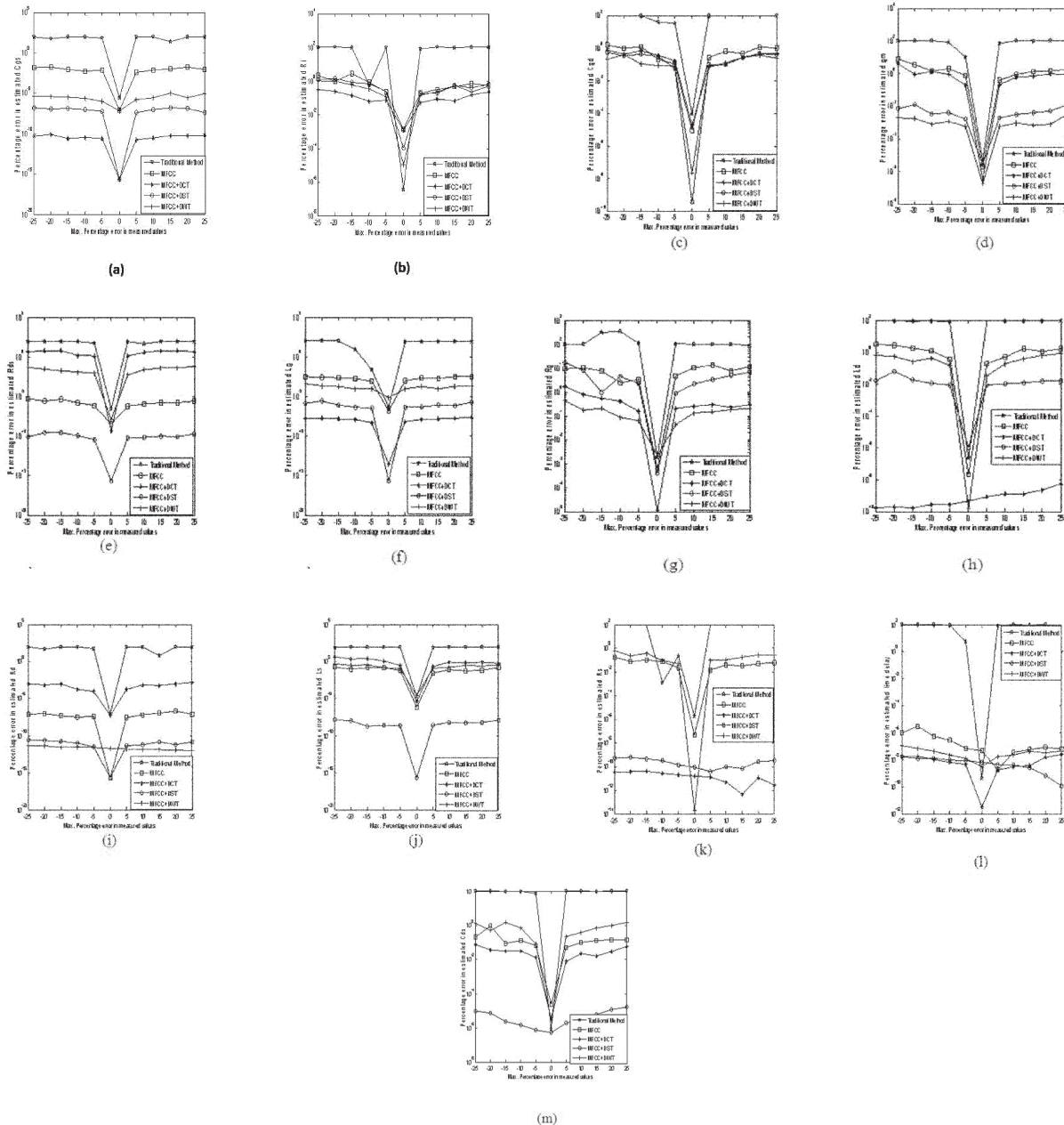


Fig. 4. Variation of the estimation error of all elements with the percentage error in measured values for all methods.

8. Conclusion

This paper presented a new approach for FET small-signal modelling. This approach is based on estimating the MFCCs of the available data set of S-parameters and frequencies and

the MFCCs of one of the discrete transforms of the data set, and using them for neural training and testing. The advantages of this approach are a reduction in the neural networks size and storage capacity, a reduction in the training time and a large immunity to measurement errors in the testing phase.

The proposed approach has been tested on published data, and succeeded to reduce the effect measurement errors on the accuracy of circuit elements estimation. All circuit models proposed for FETs can also be used, as the method is independent on the configuration of the small-signal circuit.

9. References

- [1] W. R. Curtice, and R. L. Camisa, "Self-Consistent GaAs FET Models for Amplifier Design and Device Diagnostics," *IEEE Transactions on Microwave Theory and Techniques*, Vol. MTT-32, No. 12, December, 1984.
- [2] G. D. Vendelin, M. Omori, "Circuit model for the GaAs MESFET valid to 12 GHz," *Elect. Let.*, Vol. 11, No. 3, February, 1975.
- [3] M. Berroth, and R. Bosch, "Broad-Band Determination of the FET Small-Signal Equivalent Circuit," *IEEE Transactions on Microwave Theory and Techniques*, Vol. 38, No. 7, 1990.
- [4] B. Ooi, Z. Zhong, and M. Leong, "Analytical Extraction of Extrinsic and Intrinsic FET Parameters", *IEEE Transactions on Microwave Theory and Techniques*, Vol. 57, No. 2, February, 2009.
- [5] A. Eskandanan, and S. Weinreb, "A Note on Experimental Determination of Small-Signal Equivalent Circuit of Millimeter-Wave FETs," *IEEE Transactions on Microwave Theory And Techniques*, Vol. 41, No. 1, January, 1993.
- [6] B. L. Ooi, M. S. Leong, and P. S. Kooi, "A Novel Approach for Determining the GaAs MESFET Small-Signal Equivalent-Circuit Elements", *IEEE Transactions on Microwave Theory and Techniques*, Vol. 45, No. 12, December, 1997.
- [7] A. Jarndal, and G. Kompa, "A New Small-Signal Modelling Approach Applied to GaN Devices," *IEEE Transactions on Microwave Theory and Techniques*, Vol. 53, No. 11, November 2005.
- [8] K. Shirakawa, H. Oikawa, T. Shimura, Y. Kawasaki, Y. Ohashi, T. Saito, and Y. Daido, "An Approach to Determining an Equivalent Circuit for HEMT's," *IEEE Transactions on Microwave Theory and Techniques*, Vol. 43, No. 3, March, 1995.
- [9] M. Lázaro, I. Santamaría, and C. Pantaleón, "Neural Networks for Large- and Small-Signal Modelling of MESFET/HEMT Transistors", *IEEE Trans. on Instrum. and Measurement*, Vol. 50, No. 6, December, 2001.
- [10] V. Devabhaktuni, M. Yagoub, and Q. Zhang, "A Robust Algorithm For Automatic Development Of Neural-Network Models For Microwave Applications", *IEEE Trans. on Microwave Theory and Techniques*, Vol. 49, No. 12, December, 2001.
- [11] K. Shirakawa, M. Shimiz, N. Okubo, and Y. Daido, "A Large-Signal Characterization of an HEMT Using a Multilayered Neural Network," *IEEE Transactions on Microwave Theory and Techniques*, Vol. 45, No. 9, September, 1997.
- [12] A. I. Galushkin, *Neural Networks Theory*, Springer-Verlag Berlin Heidelberg 2007.
- [13] G. Dreyfus, *Neural Networks Methodology and Applications*, Springer-Verlag Berlin Heidelberg 2005.
- [14] P. Guillemain and R. K. Martinet, "Characterization of Acoustic Signals through Continuous Linear Time-Frequency Representations", *Proceedings of the IEEE*, vol. 84, No. 4, pp. 561- 585, April 1996.
- [15] A. Prochazka, J. Uhler, P. J. W. Rayner, and N. J. Kingsbury, *Signal Analysis and Prediction*. Birkhauser Inc., 1998.
- [16] G. W. Wornell, "Emerging Applications of Multirate Signal Processing and Wavelets in Digital Communications", *Proc. of the IEEE*, vol. 84, No. 4, pp. 586-603, April 1996.
- [17] I. Daubechies, "Where Do Wavelets Come From? A Personal Point of View", *Proceedings of the IEEE*, Vol. 84, No. 4, pp. 510- 513, 1996.
- [18] A. Cohen and J. Kovacevec, "Wavelets: The Mathematical Background", *Proceedings of the IEEE*, Vol. 84, No. 4, pp. 514- 522, 1996.
- [19] N. H. Nielsen and M. V. Wickerhauser, "Wavelets and Time-Frequency Analysis", *Proceedings of the IEEE*, Vol. 84, No. 4, pp. 523- 522-540, 1996.
- [20] K. Ramchndran, M. Vetterli and C. Herley, "Wavelets, Subband Coding, and Best Basis", *Proceedings of the IEEE*, Vol. 84, No. 4, pp. 541- 560, 1996.
- [21] P. Guillemain and R. K. Martinet, "Characterization of Acoustic Signals Through Continuous Linear Time-Frequency Representations", *Proceedings of the IEEE*, Vol. 84, No. 4, pp. 561- 585, 1996.
- [22] G. W. Wornell, "Emerging Applications of Multirate Signal Processing and Wavelets in Digital Communications," *Proceedings of the IEEE*, Vol. 84, No. 4, pp. 586- 603, 1996.
- [23] S. Mallat, "Wavelets For A Vision", *Proceedings of the IEEE*, Vol. 84, No. 4, pp. 604- 614, 1996.
- [24] P. Schroder, "Wavelets in Computer Graphics," *Proceedings of the IEEE*, Vol. 84, No. 4, pp. 615- 625, 1996.
- [25] M. Unser and A. Aldroubi, "A Review of Wavelets in Biomedical Applications", *Proceedings of the IEEE*, Vol. 84, No. 4, pp. 626- 638, 1996.
- [26] M. Farge, N. Kevlahan, V. Perrier and E. Goirand, "Wavelets and Turbulence", *Proceedings of the IEEE*, Vol. 84, No. 4, pp. 639-669 , 1996.
- [27] A. Bijaoui, E. Slezak, F. Rue and E. Lega, "Wavelets and The Study of The Distant Universe", *Proceedings of the IEEE*, Vol. 84, No. 4, pp. 670- 679, 1996.
- [28] W. Sweldens, "Wavelets: What Next?", *Proceedings of the IEEE*, Vol. 84, No. 4, pp. 680- 685, 1996.
- [29] A. Prochazka, J. Uhler, P. J. W. Rayner and N. J. Kingsbury, *Signal Analysis and Prediction*. Birkhauser Inc. , 1998.
- [30] J. S. Walker, *A Primer on Wavelets and Their Scientific Applications*, CRC Press LLC, 1999.
- [31] T. Kinnunen, "Spectral Features For Automatic Text-Independent Speaker Recognition", Licentiate's Thesis, University of Joensuu, Finland, 2003.
- [32] R. Vergin, D. O. Shaughnessy, and A. Farhat, "Generalized Mel Frequency Cepstral Coefficients for Large-Vocabulary Speaker-Independent Continuous-Speech Recognition", *IEEE Transactions on Speech And Audio Processing*, Vol. 7, No. 5, pp. 525-532, September, 1999.